

Efficient Solid-State Photon Upconversion Enabled by Spin Inversion at Organic Semiconductor Interface

Seiichiro Izawa^{1,2} and Masahiro Hiramoto^{1,2}*

¹Institute for Molecular Science, 5-1 Higashiyama, Myodaiji, Okazaki 444-8787, Aichi, Japan, ² The Graduate University for Advanced Studies (SOKENDAI), 5-1 Higashiyama, Myodaiji, Okazaki, Aichi 444-8787, Japan.

E-mail: izawa@ims.ac.jp

Abstract

The emission of high-energy photons by low-energy photoexcitation is known as photon upconversion (UC). Efficient UC in the solid state is desirable owing to its application in photovoltaics and bio-imaging. In this study, we realized solid-state UC with 100 times higher efficiency than a conventional system by discovering a novel UC mechanism in bilayer organic semiconductor heterojunctions. The UC occurred through spin inversion during the charge separation and recombination at the interface. The key to the success was the triplet formation at the interface, as this could avoid the loss process during triplet diffusion, which is a problematic issue in conventional systems. As a result of this finding, efficient UC from near-infrared to visible light on flexible thin films under LED light excitation was made possible.

Main text

Photon upconversion (UC) is a process that captures low-energy photons and re-emits high-energy photons through a sequence of energy transfer steps. The potential applications of UC include the recovery of wasted low-energy photons for photovoltaics and photocatalysis, as well as bio-sensing

and photodynamic therapy using near-infrared (NIR) light, which offers the advantage of high penetration in living tissues.¹ Among the numerous UC mechanisms, triplet–triplet annihilation (TTA) has attracted substantial attention because it can be realized by non-coherent photoexcitation such as sunlight.² The common steps of TTA UC are as follows: Firstly, a low-energy photon is absorbed and a triplet exciton is formed by intersystem crossing inside a sensitizer molecule. Subsequently, triplet energy is transferred from the sensitizer to an emitter molecule, and the TTA forms one singlet exciton with high energy. Finally, UC emission occurs in the emitter molecule. TTA UC has been studied intensively to date; however, the greatest challenge remaining is that solid-state UC, which is necessary for real device applications, is inefficient,^{3,4} with an external quantum efficiency (EQE) of less than 0.1%.⁵ Moreover, other problems such as the necessity of strong laser excitation and the use of minor metals, rare-earth or toxic elements must be overcome simultaneously.²

In this study, we realized efficient solid-state UC with 100 times higher EQE than a conventional system by discovering a novel phenomenon in which UC could be observed in bilayer organic semiconductor heterojunctions. The UC occurred through triplet formation from photogenerated free-charge recombination (**Figure 1a**). The key to this mechanism was spin inversion from a singlet to a triplet during the charge separation and recombination at the interface. As a result of this novel mechanism, efficient UC from near-infrared to visible light on flexible thin films without minor metals, rare-earth or toxic elements by LED excitation was made possible.

Figure 2a presents an image of UC emission from rubrene/Y6 bilayers by 850 nm LED irradiation. Rubrene is a well-known TTA emitter and an electron donor, whereas Y6 has recently been developed as an efficient non-fullerene acceptor (NFA) in the field of organic photovoltaics (OPVs) and can absorb NIR light (**Figure 1c**).⁶ Bright yellow emission by NIR excitation could be observed on the bilayer. The emission spectrum of the rubrene/Y6 bilayer film in **Figure 2b** had the same shape as the rubrene photoluminescence (PL) in **Figure 1c**. Furthermore, the pristine rubrene film did not exhibit any emission peaks upon 850 nm LED irradiation. Therefore, the emission with a peak top of 565 nm by the 850 nm irradiation in the rubrene/Y6 bilayer film was certainly UC emission originating from the donor/acceptor (D/A) interface. The value of the apparent anti-Stokes shift, i.e. energy difference

between the lowest energy absorption peak of the sensitizer and emission peak of the emitter, was high, at 0.71 eV.

The excitation intensity dependences of the UC emission were investigated on rubrene/Y6 and rubrene/ITIC-Cl, which is another NFA.⁷ The results of the bilayer films in **Figure 3a** followed the typical tendency of TTA UC. The UC emission increased quadratically at lower excitation intensities, whereas it increased linearly at higher intensities because TTA became the main decay channel under the high triplet concentration condition.⁸ The intersection of the two fitted lines represents the threshold intensity of the UC (I_{th}), and I_{th} of the rubrene/Y6 and rubrene/ITIC-Cl bilayer films were 70.6 and 111 mW/cm², respectively. These values were smaller than those of conventional UC systems.¹ The internal quantum efficiencies (IQEs) of the UC emission on the bilayer films were calculated using the rubrene PL as a reference. The IQEs of the rubrene/Y6 and rubrene/ITIC-Cl in the saturated region were 0.57% and 1.58%, respectively.

To boost the UC efficiency further, the emissive dopant DBP was introduced into the rubrene layer by means of the co-deposition technique.⁹ The peak top shifted from 565 nm in the undoped rubrene/ITIC-Cl film to 606 nm in the 0.5% DBP-doped bilayer film owing to the energy transfer from the rubrene to the DBP. The calculated IQE of the 0.5% DBP-doped bilayer film in the saturation region was 2.53%. This increase in the IQE by DBP doping was a result of the absolute PL quantum yield of the emitter layer increasing from 39.7% in the pristine rubrene film to 71.2% in the 0.5% DBP-doped film. In particular, the EQE of the UC in the rubrene + 0.5% DBP/ITIC-Cl film was very high, namely 2.30% at 152 mW/cm², which was more than 100 times more efficient under a smaller excitation intensity than that of recently reported solid-state UC systems.⁵ This was because of the large absorbance of the NFA layer as well as the high IQE in the novel system.

To elucidate the UC mechanism at the D/A interface, the UC emission under different applied voltages was investigated in a photovoltaic device with a rubrene/ITIC-Cl bilayer as the active layer. UC emission excited by 750 nm LED irradiation was clearly observed at 0.94 V, which was the open-circuit condition (OC) of the device, as illustrated in **Figure 4a**. It was steeply quenched under a smaller applied voltage than the OC. The reason for the quenching was that photogenerated charges

were extracted to the electrode under a smaller voltage than the OC. The results demonstrated that the origin of the UC emission was photogenerated charge recombination at the D/A interface. The peak intensity of the UC emission was plotted in the same graph as the $J-V$ curve of the rubrene/ITIC-Cl bilayer photovoltaic device under 1 sun irradiation, as illustrated in **Figure 4b**. We observed a difference in the voltage dependence: the photocurrent increased continuously even under a negative bias voltage, whereas the UC emission was almost quenched at less than +0.5 V. Charge recombination in OPVs can be classified as geminate recombination (GR) from the charge transfer (CT) state, which is Coulombically bounded at the D/A interface prior to complete free charge separation, and bimolecular recombination (BR) from free charges.¹⁰ GR exhibits strong voltage dependence even in the negative voltage region, whereas BR is the dominant recombination mechanism near the OC.¹¹ Therefore, steep quenching near the OC strongly suggests that the origin of the UC at the interface was BR from free charges.

The novel UC mechanism at the interface according to the experimental results is depicted in **Figure 4d**. Firstly, the S_1 excitons that were formed following the absorption of low-energy photons in the NFA sensitizer layer were separated to the CT state at the D/A interface using the HOMO energy offset between the rubrene and NFAs (**Figure 1d**). Note that the CT state had two spin states: singlet and triplet, which are denoted as CT_1 and CT_3 , respectively.¹² The CT state formed immediately following charge separation was CT_1 owing to the spin-selection rule and the GR from CT_1 did not contribute to UC emission, as discussed in the previous paragraph. Subsequently, charge pairs were separated to form free charges with a random spin state. The process thus far was exactly the same as the photoconversion mechanism of OPVs. However, in contrast to OPVs, the bilayer films did not have electrodes; thus, the free charges eventually recombined to form a CT state again. The CT_1 and CT_3 formation rates were 25% and 75%, respectively, owing to the spin-selection statistics of free charge recombination.¹² The energy of CT_3 could be transferred to T_1 of the rubrene, following which the TTA formed S_1 , and finally, high-energy UC emission from the rubrene layer could be observed. The key process of the novel UC system was triplet formation by spin inversion of the CT state during

charge separation and recombination at the D/A interface (**Figure 4d**), whereas the triplet is formed by intersystem crossing in the sensitizer molecule in conventional UC (**Figure 4c**).

This critical difference in the mechanism solves the problems of conventional solid-state UC. The solid-state UCs reported to date have been inefficient as a result of non-radiative triplet annihilation occurring in the sensitizer layer during inefficient triplet diffusion.⁵ To avoid these loss pathways, in most cases, the sensitizer is dispersed in matrix materials.^{3,4} However, the dispersion decreases the absorbance of the sensitizer layer significantly. In contrast to conventional UC, in the novel UC system, the excited state diffusing in the sensitizer layer was a singlet, and a triplet was only formed in the emitter layer near the D/A interface. Therefore, triplet loss never occurred in the sensitizer layer, which means that a pristine film with a large absorbance could be used for the sensitizer. As a result, about 90% of incident photons were absorbed in the Rub/ITIC-Cl bilayer, whereas only a small percentage can be utilized in dispersed films in conventional UC systems.⁵ This difference as well as the high IQE resulted in a 100 times increase in the EQE in the novel UC system compared to conventional systems.

Furthermore, the triplet formation at the D/A interface means that intersystem crossing inside sensitizer molecules by the heavy atom effect is unnecessary for UC. The sensitizer molecules used in this study did not contain minor metals, rare-earth, or toxic elements, such as Pd, Ir, Pt, Yb, Os, Cd, or Pb.¹ This finding is a paradigm shift for UC because a large variety of “normal organic semiconductor materials” that have already been developed for organic electronics applications can be used to realize UC provided that the energy levels of the materials meet the requirements for each energy transfer step.

Moreover, triplet formation by charge separation and recombination offers the advantage of a small energy loss in UC because recent reports have proven that charge separation is possible with a minimized energy difference between S_1 and the CT state of less than 50 meV,¹³⁻¹⁵ which is far smaller than the typical energy loss for intersystem crossing of approximately 0.3 eV.² Our results support this point as the CT state emission in the rubrene/Y6 OLED device almost overlapped with the S_1 emission of Y6, indicating that the energy difference between S_1 and the CT state was negligible. This enabled

a small total energy loss in the UC: the energy difference of the emission peak top between S_1 of the Y6 and T_1 of the rubrene was only 0.14 eV.¹⁶

Finally, efficient UC in the bilayer thin film enabled the demonstration of bright yellow UC emission on a flexible substrate by NIR LED excitation, as depicted in **Figure 4e**. UC on flexible thin films is important for future applications in flexible solar cells, as well as bio-imaging or optogenetics applications in living organisms. Furthermore, strong laser excitation is not necessary in this system because a high EQE can be achieved under a small excitation power density. We anticipate that the significant advances of our findings will expand the applicability of UC and open a new research field based on spin inversion at the organic semiconductor interface.

Acknowledgements

This research was supported in part by JSPS KAKENHI, Grant-in-Aid for Young Scientists (18K14115), Mazda foundation and the Kao Foundation for Arts and Sciences. The authors are grateful to Mr. Tadashi Ueda at Instrument Center in Institute for Molecular Science for assistance with most of the optical measurements.

Author contributions

S.I. directed the project, conceived the idea, designed and performed the experiments, and wrote the paper. M.H. supervised the research. All of the authors reviewed the manuscript.

References

1. Zhou, J., Liu, Q., Feng, W., Sun, Y. & Li, F. Upconversion luminescent materials: advances and applications. *Chem Rev* **115**, 395-465 (2015).
2. Yanai, N. & Kimizuka, N. New Triplet Sensitization Routes for Photon Upconversion: Thermally Activated Delayed Fluorescence Molecules, Inorganic Nanocrystals, and Singlet-to-Triplet Absorption. *Acc Chem Res* **50**, 2487-2495 (2017).
3. Joarder, B., Yanai, N. & Kimizuka, N. Solid-State Photon Upconversion Materials: Structural Integrity and Triplet-Singlet Dual Energy Migration. *J Phys Chem Lett* **9**, 4613-4624 (2018).
4. Gray, V., Moth-Poulsen, K., Albinsson, B. & Abrahamsson, M. Towards efficient solid-state triplet-triplet annihilation based photon upconversion: Supramolecular, macromolecular and self-assembled systems. *Coord Chem Rev* **362**, 54-71 (2018).
5. Lin, T.A., Perkinson, C.F. & Baldo, M.A. Strategies for High-Performance Solid-State Triplet-Triplet-Annihilation-Based Photon Upconversion. *Adv Mater* **32**, e1908175 (2020).
6. Yuan, J., *et al.* Single-Junction Organic Solar Cell with over 15% Efficiency Using Fused-Ring Acceptor with Electron-Deficient Core. *Joule* **3**, 1140-1151 (2019).
7. Zhang, H., *et al.* Over 14% Efficiency in Organic Solar Cells Enabled by Chlorinated Nonfullerene Small-Molecule Acceptors. *Adv Mater* **30**, e1800613 (2018).

8. Monguzzi, A., Mezyk, J., Scotognella, F., Tubino, R. & Meinardi, F. Upconversion-induced fluorescence in multicomponent systems: Steady-state excitation power threshold. *Phys Rev B* **78** (2008).
9. Hiramoto, M., Kikuchi, M. & Izawa, S. Parts-per-Million-Level Doping Effects in Organic Semiconductor Films and Organic Single Crystals. *Adv Mater* **31**, e1801236 (2019).
10. Clarke, T.M. & Durrant, J.R. Charge Photogeneration in Organic Solar Cells. *Chem Rev* **110**, 6736-6767 (2010).
11. Proctor, C.M., Albrecht, S., Kuik, M., Neher, D. & Nguyen, T.-Q. Overcoming Geminate Recombination and Enhancing Extraction in Solution-Processed Small Molecule Solar Cells. *Adv Energy Mater* **4**, 1400230 (2014).
12. Sarma, M. & Wong, K.T. Exciplex: An Intermolecular Charge-Transfer Approach for TADF. *ACS Appl Mater Interfaces* **10**, 19279-19304 (2018).
13. Kawashima, K., Tamai, Y., Ohkita, H., Osaka, I. & Takimiya, K. High-efficiency polymer solar cells with small photon energy loss. *Nat Commun* **6**(2015).
14. Ran, N.A., *et al.* Harvesting the Full Potential of Photons with Organic Solar Cells. *Adv Mater* **28**, 1482-1488 (2016).
15. Perdigon-Toro, L., *et al.* Barrierless Free Charge Generation in the High-Performance PM6:Y6 Bulk Heterojunction Non-Fullerene Solar Cell. *Adv Mater* **32**, e1906763 (2020).
16. Huang, Z., Simpson, D.E., Mahboub, M., Li, X. & Tang, M.L. Ligand enhanced upconversion of near-infrared photons with nanocrystal light absorbers. *Chem Sci* **7**, 4101-4104 (2016).

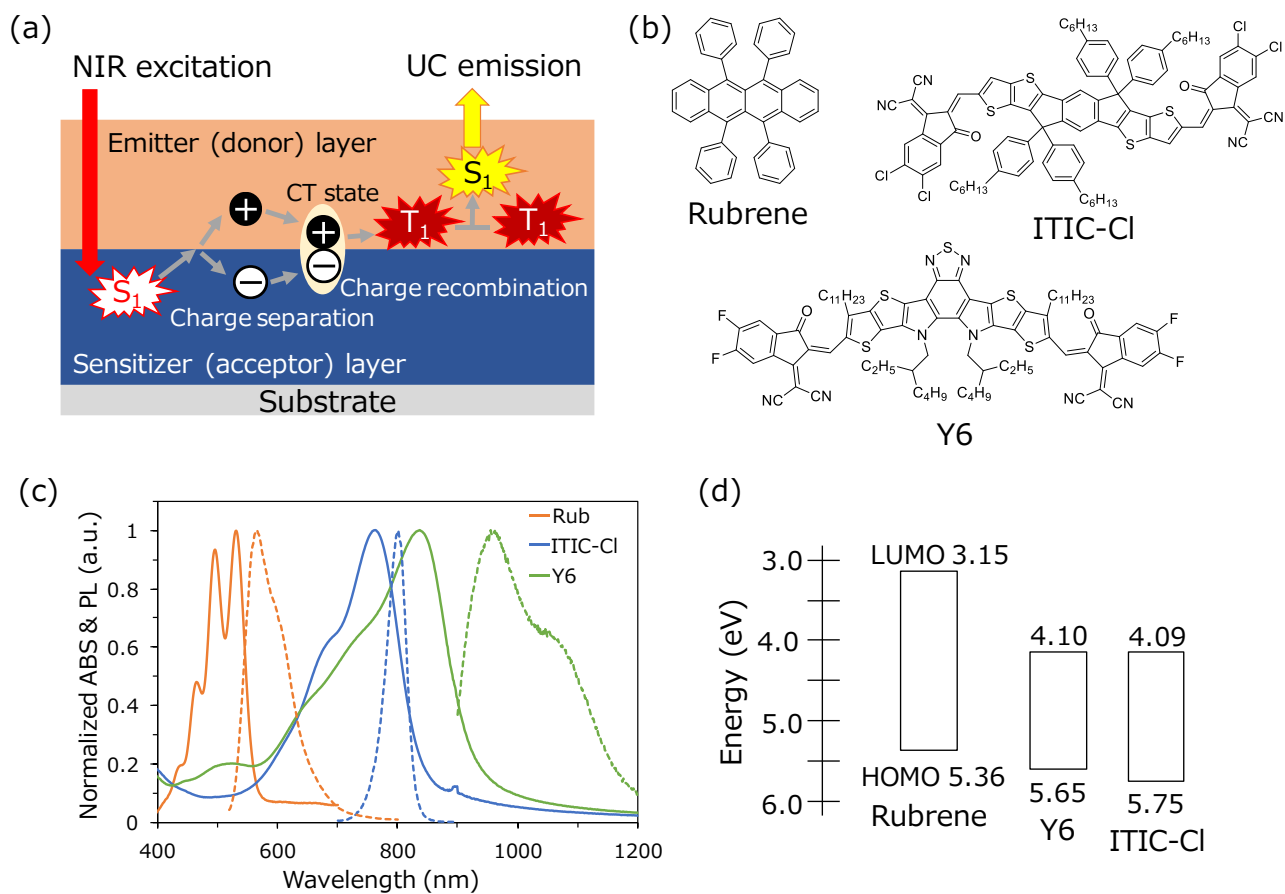


Figure 1. (a) Schematic of bilayer films and UC emission. (b) Chemical structures and (d) energy levels of rubrene, Y6, and ITIC-Cl. (c) Normalized absorption (ABS) and PL spectra of rubrene, Y6, and ITIC-Cl in thin films.

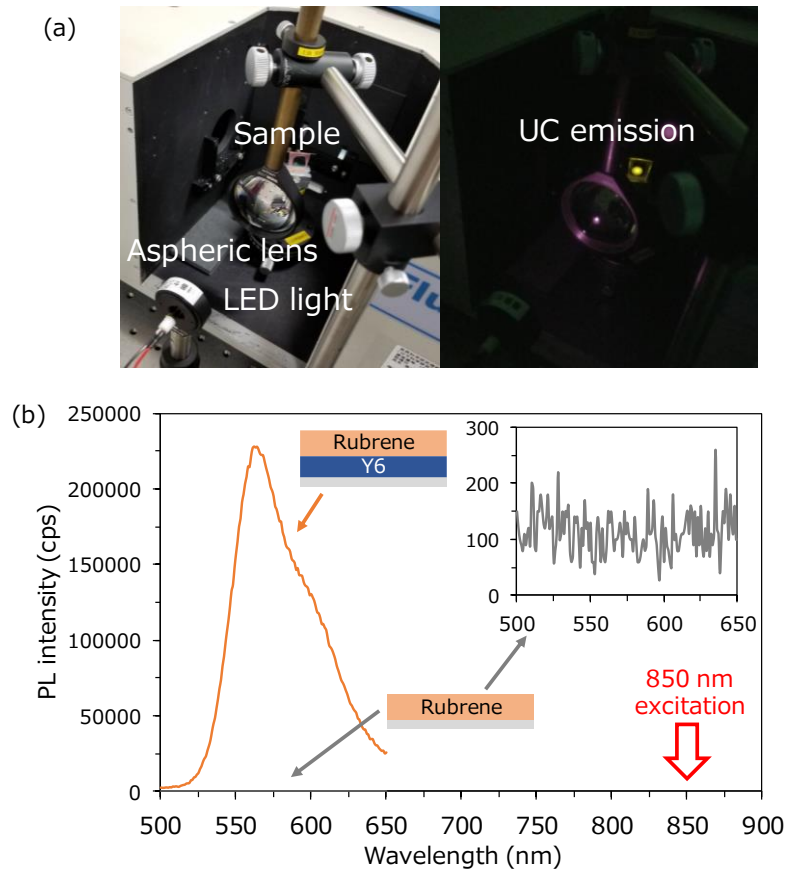


Figure 2. (a) Photograph of experimental setup in spectrofluorometer. (b) UC emission from rubrene/Y6 bilayer (orange) and pristine rubrene (gray) films irradiated by 850 nm single-color LED at power density of 108 mW/cm^2 . The inset depicts magnified views of the UC emission spectrum of the pristine rubrene film.

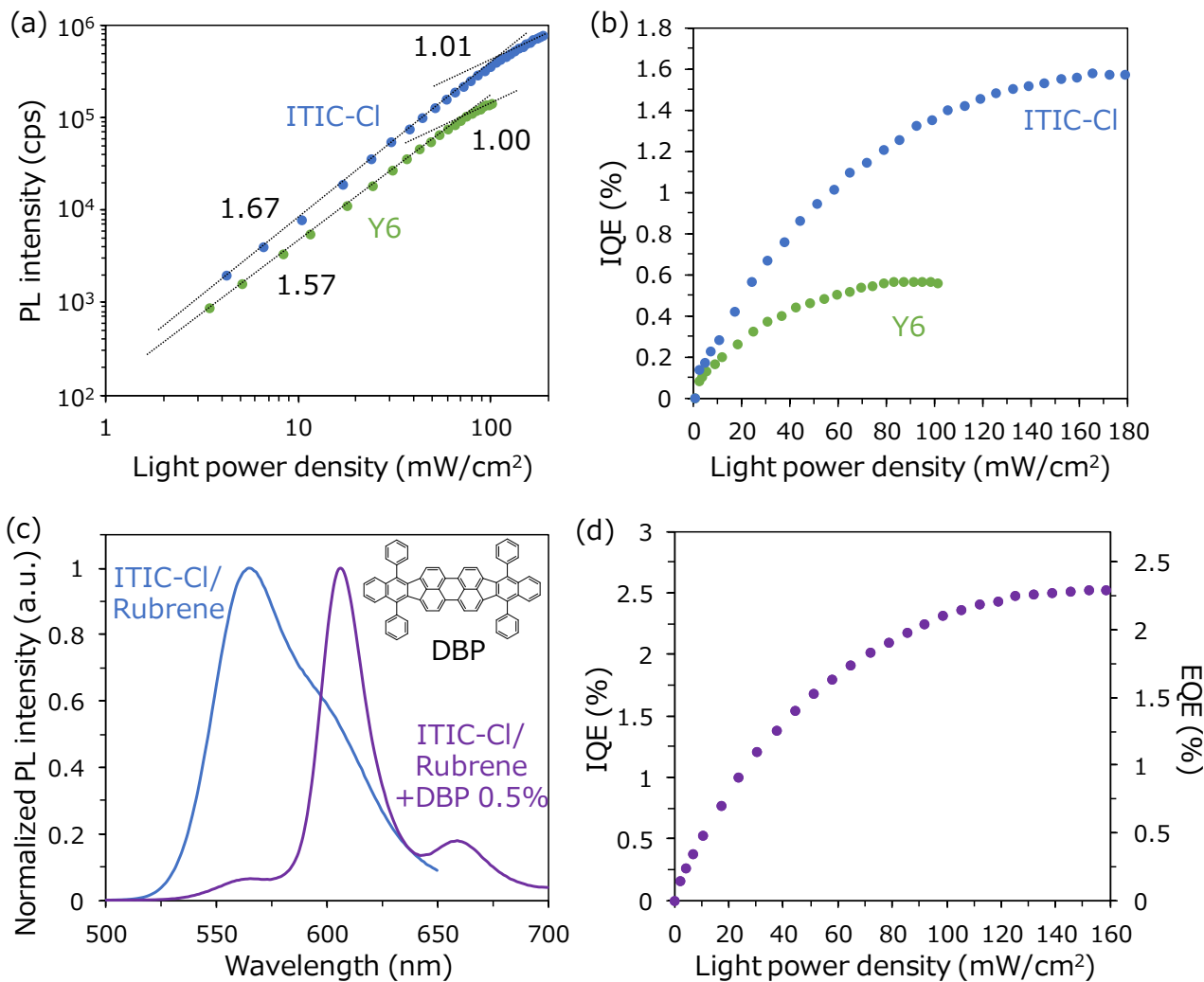


Figure 3. (a) Incident light power density dependence of UC emissions in rubrene/Y6 (green) and rubrene/ITIC-Cl (blue) bilayer films. (b) Quantum efficiency of UC emission as function of incident light power densities in rubrene/Y6 and ITIC-Cl bilayer films. (c) UC emission from rubrene/ITIC-Cl (blue) and rubrene + DBP 0.5%/ITIC-Cl (purple) bilayer films irradiated by 750 nm single-color LED at power density of 61.4 mW/cm². The inset depicts the chemical structure of DBP. (d) Quantum efficiency of UC emission as function of incident light power densities in rubrene + DBP 0.5%/ITIC-Cl bilayer film.

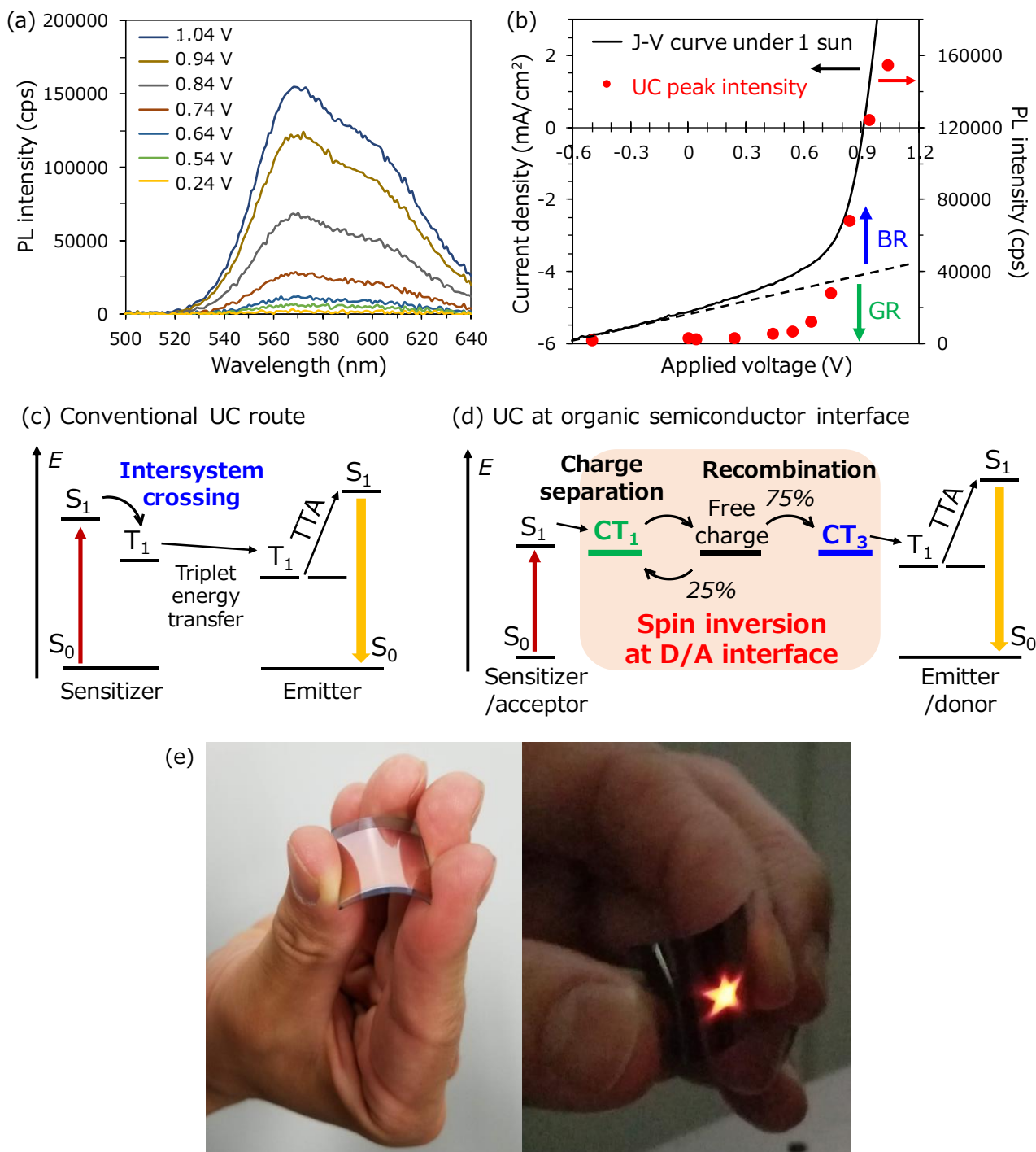


Figure 4. (a) UC emission from rubrene/ITIC-Cl bilayer photovoltaic device under applied bias, with incident light of 750 nm single-color LED at power density of 61.4 mW/cm². (b) J - V curve of rubrene/ITIC-Cl bilayer device under AM 1.5, 100 mW cm⁻² irradiation, and plot of peak intensity of Figure 4a. Schematic of mechanisms of (c) conventional UC and (d) UC at organic semiconductor interfaces. (e) Images of UC emission by patterned NIR LED irradiation (750 nm, 8.6 mW) on flexible thin film.